Supplementary Material S1

Image post-processing.

For each specimen, seven datasets were obtained corresponding to the different loading cycles. These 3D images (Figure 1-II) were registered with Fiji software [1] using the first acquired dataset as a reference to align them rigidly. Registration was performed minimizing the Euclidean difference between the reference and the target image, followed by a resampling using a cubic spline interpolation [2]. After registration, a volume of interest (VOI) was cropped for each 3D image, consisting of a parallelepiped with side lengths of 1000 voxels (2.6 mm3) in the centre of the scanned volume (Fig. 1-II, III). Noise in the images was reduced by applying a 3D median filter (radius = 2 pixels) (Fig. 1-IV). Additionally, the original SR-microCT images were also masked (Fig. 1-V) by setting to zero the voxels in the background (i.e. bone marrow). A binary image (value one for bone voxel and zero elsewhere) was first created from the filtered images using Otsu's threshold algorithm [3] followed by two cycles of closing (erosion followed by dilation), opening (dilation followed by erosion) and purifying (location of all particles in 3D and removal of all but the largest foreground and background particles [4]). These three operations removed isolated pixels and filled in small holes. The quality of the binary images was checked by visual inspection. Masked images, with the original greyscale value in the bony voxels, and zero elsewhere, were obtained multiplying the filtered to the binary images.

Evaluation of 'baseline' strains.

Methods

The evaluation of the level of uncertainties or 'baseline' stains was performed in the first two consecutive datasets for the highly- and lowly-irradiated specimens, obtained under the same constant nominal strain (0.5%), where both irradiation-induced and mechanical damage were deemed as minimal. As the images were acquired in the same deformed state, same displacement and strain fields are expected. Therefore, any non-zero values of the measured differential displacement and derived differential strain using DVC were considered as error. Six sub-volume sizes (from 16 to 112, in steps of 16 voxels), and a multi-pass scheme with a final sub-volume of 64 voxels were investigated. For each sub-volume, three different parameters were computed.

- Random errors for the differential displacement: standard deviation of each displacement component, as in [5].
- Mean absolute differential strain value: average of the average of the absolute values of the six components of the differential strain, similar to MAER or "accuracy", as in [6,7]
- Standard deviation of the differential strain value: standard deviation of the average of the absolute values of the six components of the differential strain, similar to SDER or "precision", as in [6,7].

Results

The random errors of each differential component of the displacement never exceeded 0.34 voxels (0.89 µm) for the 512 ms specimen and 0.81 voxels (2.10 µm) for the 64 ms specimen (Table S1). The

errors obtained for the displacements in the 512 ms were lower than those for the 64 ms, due to the decreased of image quality. A trend could be observed for both specimens, the higher the sub-volume size, the lower the random errors. Furthermore, the multi-pass approach reduced the random errors compared to a single-pass using the same sub-volume size.

Table S1. Random errors for the three displacement components for the highly- and lowly-irradiated specimens (512 ms and 64 ms).

Sub-volume (voxel)	**Differential displacement random errors (μm)**					
	512 ms			**64 ms**		
	X	Y	Z	X	Y	Z
16	0.78	0.75	0.84	2.11	2.08	0.86
32	0.74	0.81	0.89	1.99	1.92	0.56
48	0.69	0.66	0.79	1.99	1.86	0.41
64	0.65	0.52	0.74	1.97	1.77	0.31
80	0.60	0.41	0.69	1.90	1.59	0.23
96	0.58	0.33	0.65	1.90	1.54	0.20
112	0.62	0.33	0.65	1.93	1.57	0.20
Multipass (64)	0.62	0.38	0.60	1.96	1.68	0.24

As expected from previous studies on bone [6,8], the strain uncertainties of the DVC had decreasing trends with respect to the sub-volume size, and the values of the mean value of the differential strain were larger than the standard deviation (Fig. S1). The mean differential strain value ranged between 3856 με and 329 με for the 512 ms samples and between 6200 με and 731 με for the 64 ms sample, in sub-volumes of 16 to 112 voxels (41.6 to 291.2 μm). The standard deviation of the differential strain value ranged between 2192 με and 119 με for the 512 ms samples and between 3721 με and 269 με for the 64 ms sample, in the same sub-volumes. The multi-pass approach provided a lower level of uncertainties compared to the same sub-volume using a single-pass.

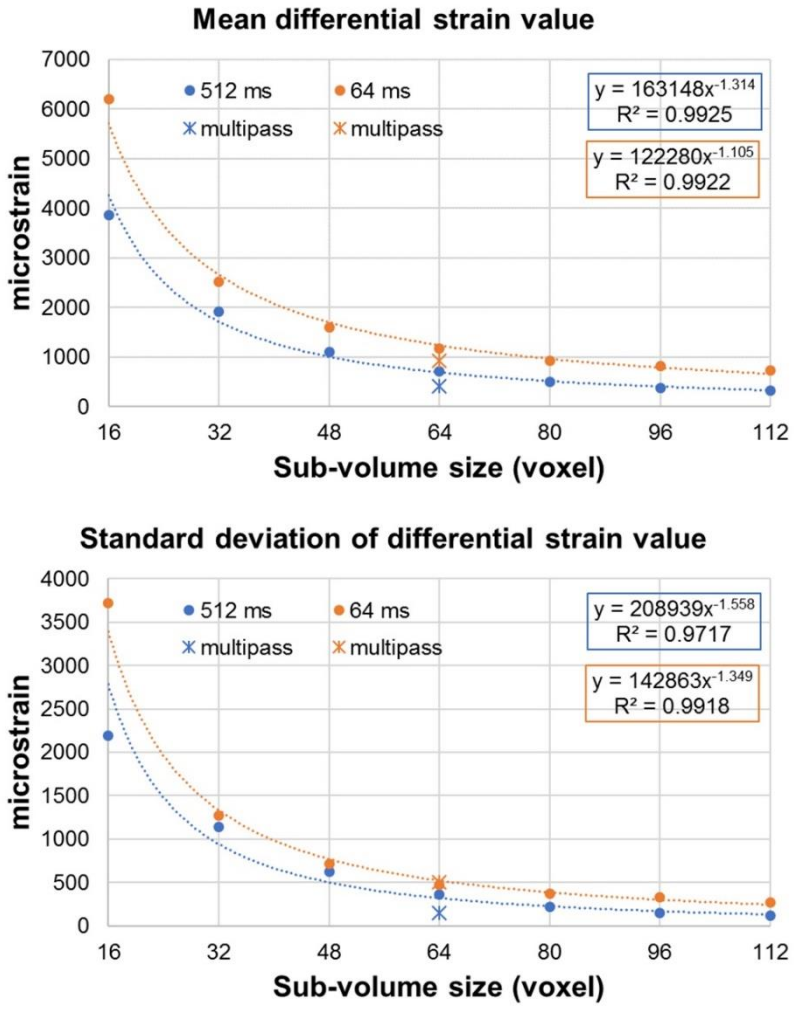

Figure S1. Relationship between the mean differential strain value (top) and standard deviation of the differential strain value (bottom) with the sub-volume size for both specimens and corresponding power laws. Power laws and coefficients of determination (R^2) are also reported.

References

[1] J. Schindelin, I. Arganda-Carreras, E. Frise, V. Kaynig, M. Longair, T. Pietzsch, S. Preibisch, C. Rueden, S. Saalfeld, B. Schmid, J.-Y. Tinevez, D.J. White, V. Hartenstein, K. Eliceiri, P. Tomancak, A. Cardona, Fiji: an open-source platform for biological-image analysis, Nat Meth. 9 (2012) 676–682. http://dx.doi.org/10.1038/nmeth.2019.

[2] E.H.W. Meijering, W.J. Niessen, M.A. Viergever, Quantitative Evaluation of Convolution-Based Methods for Medical Image Interpolation, Med. Image Anal. 5 (2001) 111–126. doi:doi.org/10.1016/S1361-8415(00)00040-2.

[3] N. Otsu, A threshold selection method from gray-level histograms, IEEE Trans. Syst. Man. Cybern. 9 (1979) 62–66. doi:10.1109/TSMC.1979.4310076.

[4] A. Odgaard, H.J.G. Gundersen, Quantification of connectivity in cancellous bone, with special emphasis on 3-D reconstructions, Bone. 14 (1993) 173–182. doi:https://doi.org/10.1016/8756-3282(93)90245-6.

[5] M. Palanca, G. Tozzi, L. Cristofolini, M. Viceconti, E. Dall'Ara, 3D Local Measurements of Bone Strain and Displacement: Comparison of Three Digital Volume Correlation Approaches., J. Biomech. Eng. 137 (2015) 1–14. doi:10.1115/1.4030174.

[6] M. Palanca, A.J. Bodey, M. Giorgi, M. Viceconti, D. Lacroix, L. Cristofolini, E. Dall'Ara, Local displacement and strain uncertainties in different bone types by digital volume correlation of synchrotron microtomograms, J. Biomech. c (2017). doi:10.1016/j.jbiomech.2017.04.007.

[7] L. Liu, E.F. Morgan, Accuracy and precision of digital volume correlation in quantifying displacements and strains in trabecular bone, J. Biomech. 40 (2007) 3516–3520. doi:10.1016/j.jbiomech.2007.04.019.

[8] E. Dall'Ara, M. Peña-Fernández, M. Palanca, M. Giorgi, L. Cristofolini, G. Tozzi, Precision of DVC approaches for strain analysis in bone imaged with μCT at different dimensional levels, Front. Mater. 4:31 (2017). doi:10.3389/fmats.2017.00031.

.